

Control-Oriented Learning of Lagrangian and Hamiltonian Systems

Mohamadreza Ahmadi, Ufuk Topcu, Clarence Rowley

Abstract—We propose a method based on quadratic programming for learning control-oriented models of physical systems for which limited data from only one trajectory is available. To this end, we take advantage of the *principle of least action*¹ from physics. We propose two methods based on quadratic programming to approximate either the Lagrangian or the Hamiltonian of the system from data. We show how these learning methods can accommodate symmetries about the underlying system, if they are known *a priori*. Furthermore, we incorporate the error in the approximation to build a data-driven differential inclusion, that is suitable for control purposes. We illustrate the results by two examples.

I. INTRODUCTION

Methods such as deep learning and reinforcement learning have been successful in modeling and controlling many dynamical systems [1], [2]. For such methods to achieve acceptable performance, we often require multiple system runs (trajectories from different initial conditions) over long time spans, i.e., large sums of data. However, for a relatively broad class of systems, collecting large sums of data can be too cumbersome or not economically efficient. The scarcity of the available data is particularly noticeable for safety-critical systems. For instance, it is not practically possible to test and collect data from all possible aircraft failure scenarios [3]. Furthermore, for safety-critical systems, we need to approximate a model that can be used for control purposes without incurring high computational cost (as opposed to conventional learning methods).

In the control literature, system analysis based on input-output data or input-state data is not new. System identification techniques [4] have looked into the problem of finding a model of the system based on data. Yet, the available methods are either data-hungry or computationally expensive (especially if they require a validation stage).

Incorporating the underlying physics of the unknown system has shown to be useful in modeling the dynamics based on trajectory data. Two recent studies in this area are [5] and [6]. Although the method in [6] extracts all physical laws that govern the system, but it requires hours of computation on multi-processor computers. The approach in [5], on the other hand, provides an algorithm to find the Lagrangian \mathcal{L} of a system from single trajectory data based on the solution to

a nonlinear optimization problem, which lacks scalability and convergence guarantees [7]. Furthermore, in [8], a method for identifying discrete Lagrangian mechanics was formulated, when the underlying dynamics evolve sufficiently close to some manifold in the configuration space. The authors also proposed a method for bounding the error bounds using techniques from reproducing kernel Hilbert spaces. Nonetheless, similar to [5] and [6], the approach in [8] also requires collecting large sum of data that may not be available in several scenarios.

Constructing Lagrangian or Hamiltonians of physical systems are important from a control perspective. In this respect, significant research has been carried out to address the control problem of Lagrangian and Hamiltonian systems [9], [10], [11], [12], [13], [14]. Most of these methods are concerned with designing tracking controllers such that the Hamiltonian has an assigned minimum corresponding to the reference trajectory. In [10, Proposition 7], an LMI formulation for stabilization is proposed based on the results of Ortega [13], [14] for linear port-Hamiltonian systems (Hamiltonian systems with inputs and outputs).

In this paper, we formulate a method based on quadratic programming to approximate the Lagrangian or the Hamiltonian of a system from limited data from a single trajectory. The proposed approach is not data hungry and, due to its quadratic programming formulation, scale very well with the number of states. If some *a priori* knowledge about the symmetries is available, we show that it can be added as a set of linear constraints to the quadratic programs. We further demonstrate how the approximation errors can be bounded and used to construct data-driven differential inclusions that can be used for control purposes, such as safety analysis [15]. We elucidate the proposed method by two examples, namely, the Duffing oscillator and the Acrobot.

The paper is organized as follows. The next section presents the notation and a brief introduction to Lagrangian and Hamiltonian mechanics. In Section III, we propose a method based on convex optimization (quadratic programming) to approximate the Lagrangian and the Hamiltonian. Section IV discusses how we can bound the approximation errors. In Section V, we formulate data-driven differential inclusions based on the approximated dynamics and the error bounds. Two examples are studied in Section VI to illustrate the proposed methods in the paper. Finally, Section VII concludes the paper and provides directions for future research.

II. PRELIMINARIES

Notation: $\mathbb{R}_{\geq 0}$ denotes the set $[0, \infty)$. $\|\cdot\|$ denotes the Euclidean vector norm on \mathbb{R}^n and $\langle \cdot \rangle$ the inner product. For

M. Ahmadi and U. Topcu are with the Department of Aerospace Engineering and Engineering Mechanics, and the Institute for Computational Engineering and Sciences (ICES), University of Texas at Austin, 201 E 24th St, Austin, TX 78712. C. Rowley is with the Department of Mechanical Engineering and Aerospace Engineering, Princeton University, Princeton, NJ 08544, e-mail: ({mrahmadi, utopcu}@utexas.edu, {crowley}@princeton.edu).

¹A system moves in such a way that the time integral over the Lagrangian takes an extreme value, i.e., $\delta \int_{t_1}^{t_2} \mathcal{L} dt = 0$.

$A \in \mathbb{R}^{m \times n}$, $A' \in \mathbb{R}^{m \times n}$ denotes its transpose and $A|_k$ its k th row. For a function $f: A \rightarrow B$, $f \in L^p(A, B)$, $1 \leq p < \infty$, implies that $(\int_A |f(t)|^p dt)^{\frac{1}{p}} < \infty$ and $\sup_{t \in A} |f(t)| < \infty$ for $p = \infty$.

A. Lagrangian and Hamiltonian Mechanics

We provide a brief introduction to Lagrangian and Hamiltonian mechanics. Our notation in the sequel follows [16] and [17].

Let $Q \subset \mathbb{R}^n$ be an n -dimensional *configuration manifold* with local coordinates $q = (q_1, q_2, \dots, q_n)'$ and TQ the corresponding *tangent bundle* (the state space). The Lagrangian $\mathcal{L}(q_1, q_2, \dots, q_n, \dot{q}_1, \dots, \dot{q}_n)$, $\mathcal{L}: TQ \rightarrow \mathbb{R}$, is a twice differentiable function that satisfies the Euler-Lagrange equations

$$\frac{d}{dt} \left(\frac{\partial \mathcal{L}}{\partial \dot{q}} \right) - \frac{\partial \mathcal{L}}{\partial q} = B(q)u, \quad (1)$$

where $B(q)u$ represents the external forces. Throughout this paper, we assume $u \in L^\infty([0, \infty), U)$, with U being the control manifold. For *simple mechanical systems*, the Lagrangian is the difference between the (positive semi-definite) kinetic energy \mathcal{K} and the potential energy \mathcal{P}

$$\mathcal{L} = \mathcal{K} - \mathcal{P}. \quad (2)$$

Given the Lagrangian, we can find the system dynamics by solving (1) for each local coordinates. The system is referred to as fully-actuated, if $\text{rank}[B(q)] = n$, and, under-actuated, if $\text{rank}[B(q)] < n$. In other words, under-actuated systems are mechanical systems that have fewer actuators than configuration variables.

At this point, let T^*Q to be the cotangent bundle of Q . The Hamiltonian is a function $\mathcal{H}: T^*Q \rightarrow \mathbb{R}$. We define the local coordinates on T^*Q to be the pair $(q, p) \in \mathbb{R}^n \times \mathbb{R}^n$, where p is referred to as the generalized momenta defined as $p_i = \frac{\partial \mathcal{L}}{\partial \dot{q}_i}$. We can calculate the Hamiltonian of the system from Lagrangian using the so called Legendre transform as

$$\mathcal{H}(q, p) = \sum_{i=1}^n \frac{\partial \mathcal{L}(q, \dot{q})}{\partial \dot{q}_i} \dot{q}_i - \mathcal{L}(q, \dot{q}). \quad (3)$$

Once the Hamiltonian is known, we can obtain the dynamics of the system as

$$\begin{bmatrix} \dot{p} \\ \dot{q} \end{bmatrix} = \begin{bmatrix} -\frac{\partial \mathcal{H}(q, p)}{\partial q} \\ \frac{\partial \mathcal{H}(q, p)}{\partial p} \end{bmatrix} + \begin{bmatrix} B(q) \\ 0 \end{bmatrix} u. \quad (4)$$

III. CONTROL-ORIENTED LEARNING VIA CONVEX OPTIMIZATION

A. Lagrangian Approximation

In this section, we propose a method for approximating the Lagrangian of a physical system from data. That is, given $\{t_i, u(t_i), q(t_i), \dot{q}(t_i), \ddot{q}(t_i)\}_{i=1}^N$, find an approximated Lagrangian $\hat{\mathcal{L}}(q, \dot{q})$ of the system. We consider the following structure

$$\hat{\mathcal{L}}(q, \dot{q}) = \sum_{i=1}^d \alpha_i \phi_i(q, \dot{q}), \quad (5)$$

where $\phi_i(q, \dot{q})$, $i = 1, \dots, d$ are a set of twice differentiable basis functions, e.g. polynomial or Chebyshev basis, and α_i , $i = 1, \dots, d$, a set of constants. Substituting (5) in (1) yields

$$\begin{aligned} & \frac{d}{dt} \left(\frac{\partial \left(\sum_{i=1}^d \alpha_i \phi_i(q, \dot{q}) \right)}{\partial \dot{q}} \right) - \frac{\partial \left(\sum_{i=1}^d \alpha_i \phi_i(q, \dot{q}) \right)}{\partial q} \\ &= \sum_{i=1}^d \alpha_i \frac{d}{dt} \left(\frac{\partial (\phi_i(q, \dot{q}))}{\partial \dot{q}} \right) - \sum_{i=1}^d \alpha_i \frac{\partial (\phi_i(q, \dot{q}))}{\partial q} \\ &= \sum_{i=1}^d \alpha_i \left(\frac{d}{dt} \left(\frac{\partial (\phi_i(q, \dot{q}))}{\partial \dot{q}} \right) - \frac{\partial (\phi_i(q, \dot{q}))}{\partial q} \right). \end{aligned} \quad (6)$$

We define the following cost function

$$\begin{aligned} J_k(\alpha, t) &:= \sum_{i=1}^d \sum_{j=1}^n \alpha_i \left(\frac{\partial^2 \phi_i(q, \dot{q})}{\partial \dot{q}_j \partial q_k} \dot{q}_k + \frac{\partial^2 \phi_i(q, \dot{q})}{\partial \dot{q}_j \partial \dot{q}_k} \ddot{q}_k \right) \\ &\quad - B(q)u(t)|_k - \sum_{i=1}^d \alpha_i \frac{\partial \phi_i(q, \dot{q})}{\partial q_k}, \quad k = 1, 2, \dots, n, \end{aligned} \quad (7)$$

where we computed the time-derivative in the last line of (6) to obtain the right-hand side of (7). Define the following aggregate objective function

$$J(\alpha) = \frac{1}{N} \sum_{i=1}^N J'(\alpha, t_i) J(\alpha, t_i),$$

where $J(\alpha, t_i) = (J_1(\alpha, t_i), \dots, J_n(\alpha, t_i))'$. Note that each $J_k(\alpha, t_i)$ is an affine function of α ; $(\cdot)^2$ is a strictly convex, non-decreasing function, and the sum of a set of convex functions is convex; hence, $J(\alpha)$ is a convex function of α . Furthermore, by the second derivative test, one can show that $J(\alpha)$ is in fact strictly convex.

Therefore, given $\{t_i, u(t_i), q(t_i), \dot{q}(t_i), \ddot{q}(t_i)\}_{i=1}^N$, it suffices to solve the following convex optimization problem to find an approximated Lagrangian

$$\min_{\alpha} J(\alpha). \quad (8)$$

Note that the above optimization problem is indeed a quadratic program, since $J(\alpha)$ is a quadratic function of the parameters α . That is, it can be written as

$$\min_{\alpha} \alpha' Q \alpha + c' \alpha$$

where Q is a positive definite matrix due to the fact that $J(\alpha)$ is a strictly convex function. Furthermore, in order to avoid the trivial solution $\hat{\mathcal{L}} = 0$ which corresponds to $\alpha \equiv 0$, without loss of generality, we add the linear constraint $\sum_{i=1}^d \alpha_i \geq \mu$, where $\mu > 0$ is a small preset constant.

For positive definite Q , the ellipsoid method can be used to solve the quadratic program in polynomial time [18]. This can be compared to the nonlinear optimization formulation solved by the Nelder-Mead method in [5], which can take an enormous amount of iterations with negligible improvement in function value [7].

B. Hamiltonian Approximation

Similar to the previous section, we now describe a method based on convex optimization to approximate the Hamiltonian from data. That is, given $\{t_i, u(t_i), q(t_i), \dot{q}(t_i), p(t_i), \dot{p}(t_i)\}_{i=1}^N$, find an approximated Hamiltonian $\mathcal{H}(q, p)$ of the system. Once this Hamiltonian is found, the estimated dynamics of the system can be found by (4).

We consider a the following parametrization for approximating the Hamiltonian

$$\hat{\mathcal{H}}(q, p) = \sum_{i=1}^d \alpha_i \phi_i(q, p). \quad (9)$$

Substituting the above parametrized Hamiltonian in (4) yields

$$\begin{aligned} \dot{p} &= - \sum_{i=1}^d \alpha_i \frac{\partial \phi_i(q, p)}{\partial q} + B(q)u, \\ \dot{q} &= + \sum_{i=1}^d \alpha_i \frac{\partial \phi_i(q, p)}{\partial p}. \end{aligned} \quad (10)$$

We also define the following functions

$$\begin{aligned} L_{k,p}(\alpha, t) &:= \dot{p}_k + \sum_{i=1}^d \alpha_i \frac{\partial \phi_i(q, p)}{\partial q_k} - B(q)u(t) \Big|_k, \\ L_{k,q}(\alpha, t) &:= \dot{q}_k - \sum_{i=1}^d \alpha_i \frac{\partial \phi_i(q, p)}{\partial p_k}, \end{aligned}$$

for $k = 1, 2, \dots, n$. Then, the following convex aggregate objective function can be defined

$$L(\alpha) = \frac{1}{N} \sum_{i=1}^N \left(L'_p(\alpha, t_i) L_p(\alpha, t_i) + L'_q(\alpha, t_i) L_q(\alpha, t_i) \right) \quad (11)$$

Then, given the data $\{t_i, u(t_i), q(t_i), \dot{q}(t_i), p(t_i), \dot{p}(t_i)\}_{i=1}^N$, it suffices to solve the following convex optimization problem to find the approximated Hamiltonian

$$\min_{\alpha} L(\alpha). \quad (12)$$

Note that, similar to (8), (12) is also a quadratic program.

C. Incorporating Symmetries: Noether's Theorem

Conservation laws are ubiquitous in physical systems. Once a conservation law about a physical system is known, the derivation of the equations describing the dynamics of the system may become less involved. An important result in physics, which relates the existence of conservation laws to symmetries², is Noether's (first) Theorem [19], i.e., every differentiable symmetry of the action of a physical system has a corresponding conservation law.

We consider three classes of symmetries:

²A symmetry is some continuous transformation of the system which leaves some physical or mathematical feature (e.g. the Lagrangian) unchanged.

- If the system is subject to *space translational symmetry* in a coordinate q_i , i.e., $\frac{\partial \mathcal{L}}{\partial q_i} = 0$, we have the conservation of momentum in that direction

$$\frac{d}{dt} \left(\frac{\partial \mathcal{L}}{\partial \dot{q}_i} \right) = \frac{dp_i}{dt} = 0. \quad (13)$$

- If the system is subject to *temporal translational symmetry*, i.e., $\frac{\partial \mathcal{L}}{\partial t} = 0$, we have the conservation of energy (Hamiltonian)

$$\frac{d}{dt} \left(\sum_{i=1}^n \frac{\partial \mathcal{L}}{\partial \dot{q}_i} \dot{q}_i - \mathcal{L} \right) = \frac{d\mathcal{H}}{dt} = 0. \quad (14)$$

- Similarly, if the system is subject to *rotational symmetry* in the generalized coordinate q_i , we can show that the angular momentum is conserved

$$\begin{aligned} \frac{d}{dt} \left(\frac{\partial \mathcal{L}}{\partial \dot{q}_i} \cdot (\vec{n} \times q_i) \right) &= \frac{d}{dt} \left(\frac{\partial \mathcal{L}}{\partial \dot{q}_i} \cdot (\vec{n} \times q_i) \right) \\ &= \frac{d}{dt} \left(\vec{n} \cdot (q_i \times \frac{\partial \mathcal{L}}{\partial \dot{q}_i}) \right) = \frac{d}{dt} \left(\vec{n} \cdot (q_i \times p_i) \right) = 0, \end{aligned} \quad (15)$$

where \vec{n} is the unit vector on the axis of rotation.

If any of the above symmetries is known *a priori* about the system, either equations (13), (14) or (15), depending on the symmetry, can be added as a linear constraint to the quadratic programs (8) and (12).

IV. BOUNDING APPROXIMATION ERRORS

Although optimization problems (8) and (12) are convex programs, their solution may not lead to the actual Lagrangian and Hamiltonian, respectively, of the system. These discrepancies are not only due to the lack of complete information about the system trajectory (limited available data), but also can result from the number of basis functions considered (and the type of basis functions e.g. polynomial, Chebyshev and etc.). Next, we delineate a method to find bounds on the approximation errors from the convex programs.

A. Lagrangian Case

We now show that the error between the approximated Lagrangian and the actual Lagrangian can be represented by an external force exerted to the system. Let $\Delta \mathcal{L}(q, \dot{q})$ denote the error in the Lagrangian estimation. We have $\mathcal{L}(q, \dot{q}) = \hat{\mathcal{L}}(q, \dot{q}) + \Delta \mathcal{L}(q, \dot{q})$. Taking the variation δ from both sides of the above equation gives

$$\begin{aligned} \delta \mathcal{L}(q, \dot{q}) &= \delta \left(\hat{\mathcal{L}}(q, \dot{q}) + \Delta \mathcal{L}(q, \dot{q}) \right) \\ &= \delta \hat{\mathcal{L}}(q, \dot{q}) + \delta \Delta \mathcal{L}(q, \dot{q}). \end{aligned} \quad (16)$$

From (1), we know that $\delta \mathcal{L}(q, \dot{q}) = B(q)u$. Therefore, we obtain

$$B(q)u = \frac{d}{dt} \left(\frac{\partial \hat{\mathcal{L}}}{\partial \dot{q}} \right) - \frac{\partial \hat{\mathcal{L}}}{\partial q} + \delta \Delta \mathcal{L}(q, \dot{q}) \quad (17)$$

That is, $-\delta\Delta\mathcal{L}(q, \dot{q}) = \frac{d}{dt} \left(\frac{\partial \hat{\mathcal{L}}}{\partial \dot{q}} \right) - \frac{\partial \hat{\mathcal{L}}}{\partial q} - Bu$. Defining $\varepsilon_L(q, \dot{q}, \ddot{q}) := -\delta\Delta\mathcal{L}(q, \dot{q}) \in \mathbb{R}^n$, we have

$$\frac{d}{dt} \left(\frac{\partial \hat{\mathcal{L}}}{\partial \dot{q}} \right) - \frac{\partial \hat{\mathcal{L}}}{\partial q} - Bu = \varepsilon_L(q, \dot{q}, \ddot{q}), \quad (18)$$

which implies that the error between the actual Lagrangian \mathcal{L} and the Lagrangian estimated from data $\hat{\mathcal{L}}$ can be characterized as an external force acting on the approximated system. Furthermore, we infer

$$\left| \frac{d}{dt} \left(\frac{\partial \hat{\mathcal{L}}}{\partial \dot{q}} \right) - \frac{\partial \hat{\mathcal{L}}}{\partial q} - Bu \right| = |\varepsilon_L(q, \dot{q}, \ddot{q})| \leq \sup_{q, \dot{q}, \ddot{q}} \varepsilon_L(q, \dot{q}, \ddot{q}), \quad (19)$$

where the supremum is element-wise. Note that if the optimal solution to problem (8) is $\gamma^* = 0$, then $\varepsilon_L|_{\{t_i, q(t_i), \dot{q}(t_i), \ddot{q}(t_i)\}_{i=1}^N} = 0$. Hence, $J(\alpha, t_i) = \varepsilon_L(q(t_i), \dot{q}(t_i), \ddot{q}(t_i))$. However, due to the finiteness of the parametrization of \mathcal{L} , γ^* is often non-zero. With $\gamma^* \neq 0$, we have

$$\begin{aligned} \frac{1}{N} \sum_{i=1}^N J'(\alpha, t_i) J(\alpha, t_i) \\ = \frac{1}{N} \sum_{i=1}^N |\varepsilon_L(q(t_i), \dot{q}(t_i), \ddot{q}(t_i))|^2 \leq \gamma^*, \end{aligned}$$

which implies $\sup_{i \in \{1, 2, \dots, N\}} |\varepsilon_L(q(t_i), \dot{q}(t_i), \ddot{q}(t_i))| \leq \sqrt{\gamma^*}$. Consequently,

$$\underline{\varepsilon}_L \leq \varepsilon_L \leq \bar{\varepsilon}_L,$$

where $\underline{\varepsilon}_L = -\sqrt{\gamma^*} \mathbf{1}_n$ and $\bar{\varepsilon}_L = \sqrt{\gamma^*} \mathbf{1}_n$.

B. Hamiltonian Case

To see the effect of the error in approximating the Hamiltonian, we substitute $\mathcal{H} = \hat{\mathcal{H}} + \Delta\mathcal{H}$ in (4) to obtain

$$\begin{bmatrix} \dot{p} \\ \dot{q} \end{bmatrix} = \begin{bmatrix} -\frac{\partial \hat{\mathcal{H}}(q, p)}{\partial q} \\ \frac{\partial \hat{\mathcal{H}}(q, p)}{\partial p} \end{bmatrix} + \begin{bmatrix} B(q) \\ 0 \end{bmatrix} u + \begin{bmatrix} -\frac{\partial \Delta\mathcal{H}(q, p)}{\partial q} \\ \frac{\partial \Delta\mathcal{H}(q, p)}{\partial p} \end{bmatrix}. \quad (20)$$

Defining $\varepsilon_H(q, p) = \begin{bmatrix} -\frac{\partial \Delta\mathcal{H}(q, p)}{\partial q} \\ \frac{\partial \Delta\mathcal{H}(q, p)}{\partial p} \end{bmatrix}$, we have

$$\begin{bmatrix} \dot{p} \\ \dot{q} \end{bmatrix} = \begin{bmatrix} -\frac{\partial \hat{\mathcal{H}}(q, p)}{\partial q} \\ \frac{\partial \hat{\mathcal{H}}(q, p)}{\partial p} \end{bmatrix} + \begin{bmatrix} B(q) \\ 0 \end{bmatrix} u + \varepsilon_H. \quad (21)$$

Therefore, the influence of the error in Hamiltonian approximation can be viewed as the model being subject to the disturbance ε_H . Let γ^* be the solution to quadratic program (12) with $L(\alpha)$ defined as (11). Then, we have

$$\frac{1}{N} \sum_{i=1}^N \left(L'_p(\alpha, t_i) L_p(\alpha, t_i) + L'_q(\alpha, t_i) L_q(\alpha, t_i) \right) \leq \gamma^*,$$

which in turn implies that

$$\sup_{i \in \{1, \dots, N\}} (|L_p(\alpha, t_i)|^2 + |L_q(\alpha, t_i)|^2) \leq \gamma^*.$$

Without loss of generality, we assume the error is divided equally between the p and q dynamics.

That is, to say $\sup_{i \in \{1, \dots, N\}} |L_p(\alpha, t_i)|^2 \leq \frac{\gamma^*}{2}$ and $\sup_{i \in \{1, \dots, N\}} |L_q(\alpha, t_i)|^2 \leq \frac{\gamma^*}{2}$. Then, following the same lines as of the derivation detailed in the previous section, we obtain

$$\underline{\varepsilon}_H \leq \varepsilon_H \leq \bar{\varepsilon}_H,$$

with $\underline{\varepsilon}_H = -\sqrt{\frac{\gamma^*}{2}} \mathbf{1}_{2n}$ and $\bar{\varepsilon}_H = \sqrt{\frac{\gamma^*}{2}} \mathbf{1}_{2n}$.

V. DATA-DRIVEN DIFFERENTIAL INCLUSIONS

In this section, we build differential inclusion descriptions of the system dynamics using the approximated Lagrangian (as described in Section III-A) and the approximated Hamiltonian (as described in Section III-B).

A. Lagrangian System

Given the approximated $\hat{\mathcal{L}}$ in the form of (5), we can estimate the underlying dynamics as

$$M(q, \dot{q}) \ddot{q} + C(q, \dot{q}) \dot{q} + V(q, \dot{q}) = B(q)u, \quad (22)$$

where

$$M_{kj} = \sum_{i=1}^d \alpha_i \frac{\partial^2 \phi_i(q, \dot{q})}{\partial \dot{q}_j \partial \dot{q}_k}, \quad (j, k) \in \{1, 2, \dots, n\}^2,$$

is a symmetric matrix, and

$$C_{kj} = \sum_{i=1}^d \alpha_i \frac{\partial^2 \phi_i(q, \dot{q})}{\partial \dot{q}_j \partial q_k}, \quad (j, k) \in \{1, 2, \dots, n\}^2,$$

$$V_k = -\sum_{i=1}^d \alpha_i \frac{\partial \phi_i(q, \dot{q})}{\partial q_k}, \quad k \in \{1, 2, \dots, n\}.$$

For physical systems, the matrix M is called the inertial matrix and M is positive definite and symmetric [20, Chapter 4]. Multiplying both sides of (22) from left by M^{-1} , we have

$$\begin{aligned} \ddot{q} = & -M^{-1}(q, \dot{q})C(q, \dot{q}) \dot{q} \\ & - M^{-1}(q, \dot{q})V(q, \dot{q}) + M^{-1}(q, \dot{q})B(q)u. \end{aligned} \quad (23)$$

Taking into account the error in approximating the Lagrangian and using a construction analogous to [15], we obtain

$$\ddot{q} \in \text{co}\{F\}(q, \dot{q}, u), \quad t \geq t_N, \quad (24)$$

subject to the initial conditions $q(t_N)$ and $\dot{q}(t_N)$, where the set-valued map $F : TQ \times U \rightarrow 2^{TQ}$ is given by

$$\begin{aligned} F : (q, \dot{q}) \mapsto & -M^{-1}(q, \dot{q})C(q, \dot{q}) \dot{q} - M^{-1}(q, \dot{q})V(q, \dot{q}) \\ & + M^{-1}(q, \dot{q})B(q)u + M^{-1}\varepsilon_L, \\ & \varepsilon_L \in (\underline{\varepsilon}_L, \bar{\varepsilon}_L), \end{aligned} \quad (25)$$

where the bounds $\underline{\varepsilon}_L$ and $\bar{\varepsilon}_L$ are computed as described in Section IV-A.

Figure 1 illustrates the solution set of the differential inclusion (24) for a system with 1-dimensional configuration space and constant inertial matrix M . In Appendix A, we compute how the error bounds evolve with respect to $t \geq t_N$. In general, these bounds grow exponentially with time. However, the error growth can be mitigated by several

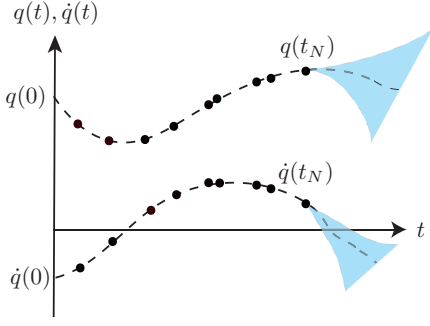


Fig. 1: Data samples (black dots), actual system trajectory (dashed lines), and the solution set of the data driven differential inclusion (blue).

factors, such as increasing the number of basis functions, increasing the number of data samples, and choosing an interpolant with least Lipschitz constant. In the examples, we show that if the approximation error is sufficiently small, these errors remain within acceptable limits depending on the number of data samples.

Next, we show that differential inclusion (24) admits solutions. We first posit the following.

Assumption 1: For $T \geq t_N$, there exists a function $C \in L^1([t_N, T], \mathbb{R}^n)$ such that $|\text{co}\{F\}(\cdot, \cdot, t)| \leq C(t)$ for all $t \in [t_N, T]$.

Proposition 1: Let $T \geq t_N$ and Assumption 1 hold. Then there exists a unique (absolutely continuous) solution to the data-driven differential inclusion (24) on $[t_N, T]$.

Proof: See Appendix B. ■

Note that Assumption 1 implies that differential inclusion (24) does not have solutions that blow-up in finite-time. Indeed, in order for the data-driven differential inclusion (24) to have solutions, we consider Lagrangian systems that do not have solutions that blow up in finite time.

B. Hamiltonian System

Similar to the previous section, we can obtain a differential inclusion corresponding to (21). That is,

$$\begin{bmatrix} \dot{p} \\ \dot{q} \end{bmatrix} \in \text{co}\{G\}(q, p, u), \quad t \geq t_N, \quad (26)$$

subject to $p(t_N)$ and $q(t_N)$, where the set valued map $G : T^*Q \times U \rightarrow 2^{T^*Q}$ is given by

$$G : (p, q, u) \mapsto \begin{bmatrix} -\frac{\partial \hat{H}(q,p)}{\partial q} \\ \frac{\partial \hat{H}(q,p)}{\partial p} \end{bmatrix} + \begin{bmatrix} B(q) \\ 0 \end{bmatrix} u + \varepsilon_H, \quad \varepsilon_H \in (\underline{\varepsilon}_H, \bar{\varepsilon}_H), \quad (27)$$

where the bounds $\underline{\varepsilon}_H$ and $\bar{\varepsilon}_H$ are computed as described in Section IV-B, $\frac{\partial \hat{H}(q,p)}{\partial q} = \sum_{i=1}^d \alpha_i \frac{\partial \phi_i(q,p)}{\partial q}$, and $\frac{\partial \hat{H}(q,p)}{\partial p} = \sum_{i=1}^d \alpha_i \frac{\partial \phi_i(q,p)}{\partial p}$.

At this point, we can state a proposition regarding the existence and uniqueness of solutions to (26). We need the following assumption, which parallels Assumption 1.

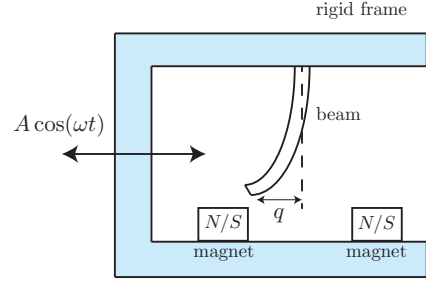


Fig. 2: The Duffing oscillator can model the deflections of a MEMS periodically forced beam which is located between two magnets.

Assumption 2: For $T \geq t_N$, there exists a function $C \in L^1([t_N, T], \mathbb{R}^n)$ such that $|\text{co}\{G\}(\cdot, \cdot, t)| \leq C(t)$ for all $t \in [t_N, T]$.

The proof of the well-posedness proposition below follows the same lines as of the proof of Proposition 1.

Proposition 2: Let $T \geq t_N$ and Assumption 2 hold. Then, the data-driven differential inclusion (26) admits a unique solutions on $[t_N, T]$.

Similar to the case of Lagrangian systems, in order to satisfy Assumption 2, we consider Hamiltonian systems that does not allow trajectories that blow up in finite time.

VI. NUMERICAL EXAMPLES

In this section, we illustrate the proposed learning methods using two examples. For illustration purposes, the basis functions we considered in both examples were polynomial functions. The differential equations were simulated using MATLAB's `ode15s` function. The corresponding convex optimization problems were solved using the parser YALMIP [23] and the solver MOSEK [24]. All computations were carried out on a Mac OS 2.5 GHz Intel Core i5 with 16 GB of RAM.

A. Example I: Duffing Oscillator

The forced Duffing equation describes oscillations subject to nonlinear elasticity. For instance, the equation models oscillations of a micro-beam which is deflected toward two magnets [25], [26] (see Figure 2). The forced Duffing equation we consider is given by

$$\begin{cases} \dot{q} = p, \\ \dot{p} = q - q^3 + 0.3 \cos(t). \end{cases} \quad (28)$$

The actual Hamiltonian of the system can be calculated as $H(q, p) = \frac{1}{2}p^2 - \frac{1}{2}q^2 + \frac{1}{4}q^4$. Note that system is not globally stable. However, it does not possess trajectories that blow up in finite time.

Consider the scenario in which we do not know the system model or the Hamiltonian *a priori*. However, we run the system from an initial configuration and collect data $\{t_i, p(t_i), q(t_i), \dot{p}(t_i), \dot{q}(t_i)\}_{i=1}^N$ (not uniformly) from time 0

TABLE I: Numerical results.

$deg(\mathcal{L})$	2	3	4	5	6
γ^*	3.100	2.1435	0.0020	0.0012	0.0009
Computing Time (s)	0.9875	1.1086	1.4307	1.8614	2.2905

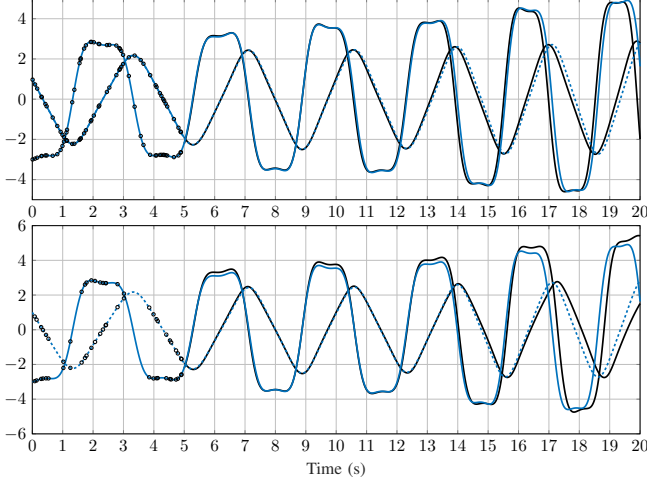


Fig. 3: The state evolutions of the Duffing oscillator (blue), the data samples (circles), and the estimated solution. $N = 50$ (top) and $N = 30$ (bottom).

to 5. Then, we compute the Hamiltonian of the system by solving quadratic program (12).

For $N = 50$, Table I shows the obtained results. We can see that, by increasing the degree of the Hamiltonian from degree 4 to 6, γ^* does not decrease significantly, but the computation time increases. Hence, we select the the model derived from the obtained Hamiltonian of degree 4 to check how the approximation error evolves over time. Figure 3 shows the data samples, the actual system trajectory, and the one obtained from the estimated Hamiltonian. Although the estimation error grows over time, but the estimation error remains within acceptable levels even 15 seconds after collecting data. In order to see the effect of N , we searched for a degree 4 Hamiltonian function when $N = 30$. As expected, Figure 3 indicates that with less data samples, the estimation error grows more rapidly.

The solutions of the data driven differential inclusion (26) can also be seen in Figure 4. The actual solution of the system remains between the two red lines. Therefore, the differential inclusion model can be used to study control properties such safety as described in [15].

One may also wonder how the algorithm performs, if we collect the same amount of data over a larger time span. Figure 5 depicts the result if we collect $N = 50$ data samples over 10 seconds instead of 5. As it is observed, the performance of the estimated model is improved if the sampling is carried out over a longer time span.

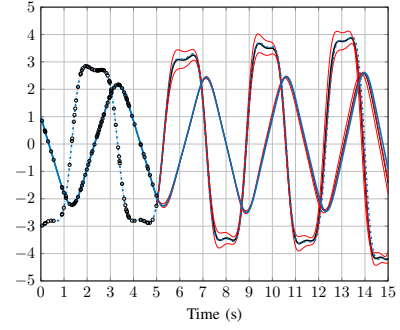


Fig. 4: The solutions of the data driven differential inclusion based on the approximated Hamiltonian (the area between the red lines).

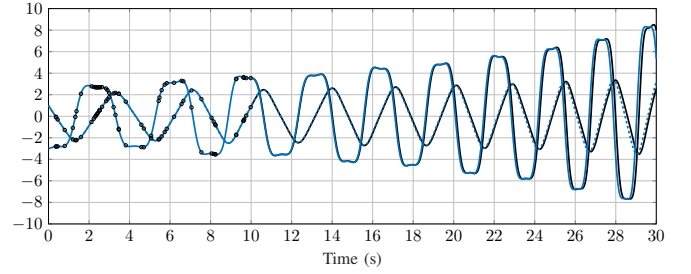


Fig. 5: The state evolutions of the Duffing oscillator (blue), the data samples (circles), and the estimated solution.

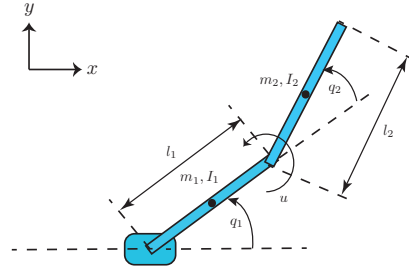


Fig. 6: The Acrobot system and the model paramters.

B. Example II: The Acrobot

The Acrobot is an under-actuated planar two-link robotic arm in the vertical plane (working against gravity), with just one actuator at the elbow [27]. It resembles a gymnast (or acrobat) on a parallel bar, who controls his/her motion by applying torque at the waist. Figure 6 illustrates the Acrobot model and the parameters.

The configuration coordinates are q_1 (the shoulder joint angle) and q_2 (the elbow relative joint angle). The actual Lagrangian of the system can be represented by (2), i.e., the difference between kinetic and potential energies, where

$$\begin{aligned} \mathcal{K} = & \frac{1}{2} I_1 \dot{q}_1^2 + \frac{1}{2} (m_2 l_1^2 + I_2 + m_2 l_1 l_2 \cos(q_2)) \dot{q}_1^2 \\ & + \frac{1}{2} I_2 \dot{q}_2^2 + \left(I_2 + \frac{m_2 l_1 l_2 \cos(q_2)}{2} \right) \dot{q}_1 \dot{q}_2, \end{aligned}$$

TABLE II: Parameters to simulate the Acrobot.

Parameter	Unit	Value
l_1	m	1
l_2	m	2
m_1	kg	1
m_2	kg	1
I_1	$kg \cdot m^2$	0.083
I_2	$kg \cdot m^2$	0.33
g	m/s^2	9.81

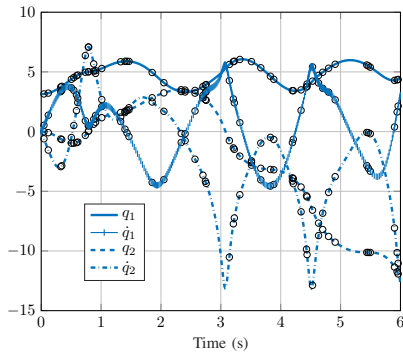


Fig. 7: The state evolutions of the Acrobot system (blue lines) and the data samples (black circles).

and

$$\mathcal{P} = \frac{m_1 g l_1 \sin(q_1)}{2} + m_2 g \left(l_1 \sin(q_1) + \frac{l_2 \sin(q_1 + q_2)}{2} \right).$$

In order to evaluate the performance of the proposed method, we simulate the dynamics of the system with the initial condition $(\pi, 0, 0, 0)'$ from time 0 to 6, using the parameter values given in Table II and then select 30 time-ordered data samples randomly to approximate the Lagrangian and then the data-driven differential inclusion (see Figure 7).

In order to approximate the dynamics, we solve optimization problem (8), subject to the matrix M as defined in (22) being positive definite for all data samples. Table III shows the obtained results. For a polynomial of degree 5, the Lagrangian has an acceptable error margin. Figure 8 illustrates the state evolution of the actual system and that of the dynamics obtained by the approximated Lagrangian for $t \geq 6$. The error margins remain relatively small for 12 seconds. However, they become more significant for $t \geq 18$.

VII. CONCLUSIONS AND FUTURE WORK

We considered the problem of estimating the Lagrangian or the Hamiltonian of a system from data, for which only limited data about one trajectory is available. The construction methods we introduced use convex optimization (quadratic

TABLE III: Numerical results.

$deg(\mathcal{L})$	2	3	4	5
γ^*	1.5032	0.2802	0.0104	0.0003
Computing Time (s)	1.0875	1.2086	1.6019	1.9814

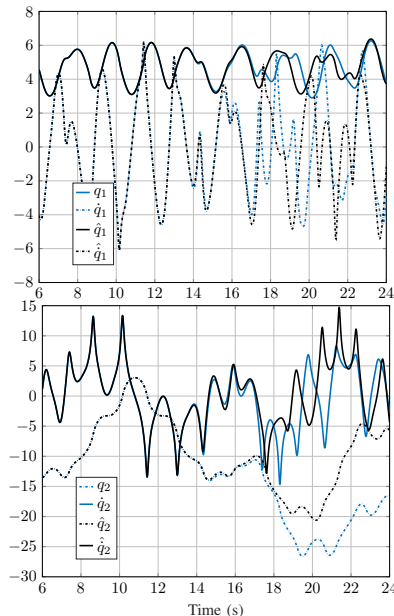


Fig. 8: The state evolutions of the Acrobot system (blue) and the approximated dynamics (black).

programming) to carry out the computations in an efficient manner. We incorporated the error in our approximations to construct data-driven differential inclusions that can be used for systems analysis and control purposes.

It was shown in the Appendix that the approximation error evolution is a function of the interpolant's Lipschitz continuity. In [28], the authors proposed a method for finding an interpolant with minimum Lipschitz constant. Adopting such interpolation techniques could further minimize the error growth. Future research will also focus on designing controller synthesis techniques based on the approximated Lagrangian and Hamiltonian functions. Such methods should carry out tasks such as tracking or stabilization along with guaranteed robustness or optimality performance. Moreover, in this paper, we assumed the data is not corrupted by noise. In many practical situations, sensor measurement errors lead naturally to measurement noise. A more practical extension of the method considered here should account for noisy data.

REFERENCES

- [1] F. L. Lewis, D. Vrabie, and K. G. Vamvoudakis, "Reinforcement learning and feedback control: Using natural decision methods to design optimal adaptive controllers," *IEEE Control Systems*, vol. 32, no. 6, pp. 76–105, 2012.
- [2] I. Lenz and A. Saxena, "Deepmpc: Learning deep latent features for model predictive control," in *In Robotics Systems and Science*, 2015.
- [3] D. Leone, "How an israeli F-15 eagle managed to land with one wing," 2014. [Online]. Available: <https://theaviationist.com/2014/09/15/f-15-lands-with-one-wing/>
- [4] L. Ljung, "Perspectives on system identification," *Annual Reviews in Control*, vol. 34, no. 1, pp. 1 – 12, 2010.
- [5] D. J. Hills, A. M. Grütter, and J. J. Hudson, "An algorithm for discovering lagrangians automatically from data," *PeerJ Computer Science*, vol. 1, p. e31, 2015.
- [6] M. Schmidt and H. Lipson, "Distilling free-form natural laws from experimental data," *Science*, no. 5923, pp. 81–85, 2009.

- [7] J. C. Lagarias, J. A. Reeds, M. H. Wright, and P. E. Wright, "Convergence properties of the Nelder–Mead simplex method in low dimensions," *SIAM Journal on Optimization*, vol. 9, no. 1, pp. 112–147, 1998.
- [8] S. Dadashi, H. G. McClelland, and A. Kurdila, "Learning theory and empirical potentials for modeling discrete mechanics," in *2017 American Control Conference (ACC)*, May 2017, pp. 4466–4472.
- [9] D. E. Chang, "Controlled lagrangian and hamiltonian systems," Ph.D. dissertation, California Institute of Technology, 2002.
- [10] S. Prajna, A. van der Schaft, and G. Meinsma, "An LMI approach to stabilization of linear port-controlled Hamiltonian systems," *Systems & Control Letters*, vol. 45, no. 5, pp. 371 – 385, 2002.
- [11] R. M. Murray, "Nonlinear control of mechanical systems: A lagrangian perspective," *Annual Reviews in Control*, vol. 21, pp. 31–45, 1997.
- [12] L. Rodrigues, "Lyapunov stability of pseudo euler-lagrange systems," in *2012 20th Mediterranean Conference on Control Automation (MED)*, July 2012, pp. 416–420.
- [13] R. Ortega, J. A. L. Perez, P. J. Nicklasson, and H. Sira-Ramirez, "Passivity-based control of euler-lagrange systems: mechanical, electrical and electromechanical applications," 2013.
- [14] R. Ortega, A. Van Der Schaft, B. Maschke, and G. Escobar, "Interconnection and damping assignment passivity-based control of port-controlled Hamiltonian systems," *Automatica*, vol. 38, no. 4, pp. 585–596, 2002.
- [15] M. Ahmadi, A. Israel, and U. Topcu, "Safety assessment for physically-viable data-driven models," in *2017 56th IEEE Conference on Decision and Control (CDC)*, Melbourne, Australia, Dec 2017.
- [16] J. E. Marsden and M. West, "Discrete mechanics and variational integrators," *Acta Numerica*, vol. 10, pp. 357–514, 2001.
- [17] J. E. Marsden and T. S. Ratiu, *Introduction to Mechanics and Symmetry: A Basic Exposition of Classical Mechanical Systems*. Springer, 2010.
- [18] S. Sahni, "Computationally related problems," *SIAM Journal on Computing*, vol. 3, no. 4, pp. 262–279, 1974.
- [19] E. Noether, "Invariante variationsprobleme," *Nachrichten von der Gesellschaft der Wissenschaften zu Gottingen, Mathematisch-Physikalische Klasse*, vol. 1918, pp. 235–257, 1918.
- [20] R. M. Murray, S. S. Sastry, and L. Zexiang, *A Mathematical Introduction to Robotic Manipulation*, 1st ed. Boca Raton, FL, USA: CRC Press, Inc., 1994.
- [21] G. Smirnov, *Introduction to the Theory of Differential Inclusions*. American Mathematical Society, 2002.
- [22] A. F. Filippov, *Differential Equations with Discontinuous Right-Hand Sides*, ser. Mathematics and Its Applications. Kluwer, 1988.
- [23] J. Lofberg, "YALMIP : a toolbox for modeling and optimization in MATLAB," in *2004 IEEE International Conference on Robotics and Automation*, 2004, pp. 284–289.
- [24] E. D. Andersen and K. D. Andersen, "The MOSEK optimization software," *EKA Consulting ApS, Denmark*, 2012.
- [25] E. Ott, *Chaos in Dynamical Systems*, 2nd ed. Cambridge University Press, 2002.
- [26] F. Tajaddodianfar, H. N. Pishkenari, M. R. H. Yazdi, and E. Maani, "On the dynamics of bistable micro/nano resonators: Analytical solution and nonlinear behavior," *Communications in Nonlinear Science and Numerical Simulation*, vol. 20, no. 3, pp. 1078 – 1089, 2015.
- [27] R. Tedrake, "Underactuated robotics: Algorithms for walking, running, swimming, flying, and manipulation," 2016, Lecture Notes. [Online]. Available: <http://underactuated.mit.edu/>
- [28] A. Herbert-Voss, M. J. Hirn, and F. McCollum, "Computing minimal interpolants in $c^{1,1}(\mathbb{R}^d)$," *Revista Matematica Iberoamericana*, vol. 33, no. 1, 2017.
- [29] J. P. Aubin and A. Celina, *Differential Inclusions*. Springer-Verlag, Berlin, 1984.

APPENDIX

A. Evolution of Error Bounds Over Time

Assuming that M is constant and invertible, for any selection of (24) (any solution for fixed ε_L), we have $co\{F\} = F$ as a single-valued map and

$$\|F(q^2, \cdot, u(t)) - F(q^1, \cdot, u(t))\| \leq l_1(t)\|q^2 - q^1\|, \quad \forall t \geq t_N,$$

and

$$\|F(\cdot, \dot{q}^2, u(t)) - F(\cdot, \dot{q}^1, u(t))\| \leq l_2(t)\|\dot{q}^2 - \dot{q}^1\|, \quad \forall t \geq t_N,$$

where $(q^i, \dot{q}^i) \in TQ$, $i = 1, 2$. For constant M , following the procedure described in [29, p. 119] using Gronwall inequality, we can show that $\|\dot{q} - \dot{q}_a\| \leq \int_{t_N}^t |M^{-1}\varepsilon_L| e^{\int_s^t l_1(\theta) d\theta} ds$, and

$$\|q - q_a\| \leq \int_{t_N}^t \left(\int_{t_N}^{\tau} |M^{-1}\varepsilon_L| e^{\int_s^{\tau} l_1(\theta) d\theta} ds \right) e^{\int_{\tau}^t l_2(\zeta) d\zeta} d\tau,$$

where $(\cdot)_a$ denotes the trajectory when $\varepsilon_L \equiv 0$. Defining $\bar{l}_1 = \sup_{t \geq t_N} l_1(t)$ and $\bar{l}_2 = \sup_{t \geq t_N} l_2(t)$, we calculate

$$\|\dot{q} - \dot{q}_a\| \leq \frac{|M^{-1}\bar{\varepsilon}_L|}{\bar{l}_1} \left(e^{\bar{l}_1(t-t_N)} - 1 \right), \quad t \geq t_N,$$

and

$$\|q - q_a\| \leq \frac{|M^{-1}\bar{\varepsilon}_L|}{\bar{l}_1} \left(\frac{e^{\bar{l}_1(t-t_N)} - e^{\bar{l}_2(t-t_N)}}{\bar{l}_1 - \bar{l}_2} + \frac{1 - e^{\bar{l}_2(t-t_N)}}{\bar{l}_2} \right)$$

when $\bar{l}_1 \neq \bar{l}_2$ and

$$\|q - q_a\| \leq \frac{|M^{-1}\bar{\varepsilon}_L|}{\bar{l}_1} \left((t-t_N)e^{\bar{l}_2(t-t_N)} - \frac{1 - e^{\bar{l}_2(t-t_N)}}{\bar{l}_2} \right),$$

when $\bar{l}_1 = \bar{l}_2$.

B. Proof of Proposition 1

The set-valued map $co\{F\}$ is defined as the convex hull of a finite set, i.e.,

$$\begin{aligned} co\{F\} = \underline{\alpha} \left(-M^{-1}(q, \dot{q})C(q, \dot{q})\dot{q} - M^{-1}(q, \dot{q})V(q, \dot{q}) \right. \\ \left. + M^{-1}(q, \dot{q})B(q)u + M^{-1}\varepsilon_L \right) \\ + \bar{\alpha} \left(-M^{-1}(q, \dot{q})C(q, \dot{q})\dot{q} - M^{-1}(q, \dot{q})V(q, \dot{q}) \right. \\ \left. + M^{-1}(q, \dot{q})B(q)u + M^{-1}\bar{\varepsilon}_L \right) \quad (29) \end{aligned}$$

with $\underline{\alpha}, \bar{\alpha} \in [0, 1]$, and $\bar{\alpha} + \underline{\alpha} = 1$. Hence, $co\{F\}$ is closed and convex. It is also measurable in t , since $u(t)$ is measurable in t and F is an affine function of u for all $t \geq t_N$. Moreover, it is an upper hemi-continuous function of q and \dot{q} , since $M > 0$ and \hat{L} is the finite weighted sum of twice differentiable bases ϕ_i . Finally, if there exist a function $C \in L^1([t_N, T], \mathbb{R}^n)$ such that $|co\{F\}(\cdot, \cdot, t)| \leq C(t)$ for all $t \in [t_N, T]$, then from [21, Theorem 4.7, p. 102], existence of solutions to (24) follows.

Furthermore, the mapping $co\{F\}$ is one-sided Lipschitz, i.e., it satisfies

$$(x_1 - x_2)' (co\{F\}(x_1, u) - co\{F\}(x_2, u)) \leq l(t)\|x_1 - x_2\|^2,$$

for some $l : \mathbb{R}_{\geq 0} \rightarrow \mathbb{R}_{\geq 0}$ and all $t \geq t_N$, x_1 and x_2 , with $x = (q, \dot{q})'$, which follows from the fact that $co\{F\}$ is a convex hull of differentiable functions and affine in $u \in L^\infty([0, T], U)$ for all $T \geq t_N$. Then, by [22, Theorem 1, p. 106], we conclude that (24) admits a unique solution.